# Monolayers having large in-plane dipole moments: Characterization of sulfone-containing self-assembled monolayers of alkanethiols on gold by Fourier transform infrared spectroscopy...

**ARTICLE** *in* LANGMUIR · NOVEMBER 1991

Impact Factor: 4.46 · DOI: 10.1021/la00059a050

# Monolayers Having Large In-Plane Dipole Moments: Characterization of Sulfone-Containing Self-Assembled Monolayers of Alkanethiols on Gold by Fourier Transform Infrared Spectroscopy, X-ray Photoelectron Spectroscopy, and Wetting

Stephen D. Evans,† Kim E. Goppert-Berarducci, Edward Urankar, Louis J. Gerenser, and Abraham Ulman*

*Corporate Research Laboratories and Analytical Technology Division, Eastman Kodak Company, Rochester, New York 14650-2109*

Robert G. Snyder

*Department of Chemistry, University of California Berkeley, California 94720*

*Received June 27, 1991*

Monolayers were formed from alkyl chain molecules having large in-plane dipole moments. The molecular species introduced was a sulfone moiety, and it was found that its incorporation strongly affected the molecular conformation within the monolayer. The effect of varying the position of the sulfone group in an otherwise straight alkyl chain, while constant molecular length was maintained, was studied, and the results were compared to those found for an octadecanethiol (ODT). The monolayers were characterized by Fourier transform infrared reflection absorption spectroscopy and X-ray photoelectron spectroscopy and by their wetting properties.

## Introduction

Recently, we reported on the effect of incorporating bulky polar groups into self-assembled alkanethiol monolayers.[1,2] During that study, in which large dipole moments were introduced *perpendicular to the plane* of the monolayer, it became evident that dipoles which acted *in the plane* of the film might present interesting physical properties in terms of molecular order and packing. It was of particular interest to observe the effect of introducing sulfone ($SO_2$) groups into otherwise straight chain alkanethiol monolayers, since these were at the center of our earlier studies involving chromophores.[3] The sulfone group has a large in-plane dipole moment, of the order of 1.6 D, which when coupled with its shape, O–S–O angle of ~109°, might induce a preferred orientation on neighboring molecules (Figure 1). Evidence to suggest this was seen in molecular dynamics (MD) simulations in the earlier studies.[4] However, this could not be unambiguously assigned to the sulfone due to additional complicating factors such as the bulky phenyl rings etc.

The motivation of the studies presented here, therefore, was to understand the effect of intermolecular electrostatic interactions *in the monolayer plane* on the packing and ordering in the assembly. Thus, while we hoped to understand further the results in our previous investigations,[1] we are interested in the more general problem of controlling order in molecular materials. In such materials, ordering is introduced through, for example, van der Waals and electrostatic interactions and H bonding. While van der Waals interactions have no specific orientation in space,

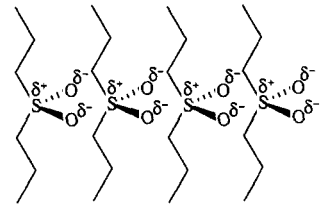

**Figure 1.** Proposed interaction between sulfone groups in two-dimensional assemblies.

one could assume that electrostatic interactions between functional groups such as the $SO_2$ group introduce well-defined orientation of dipole moments, similar to that in ferroelectric materials. Such well-defined assembly of dipoles was recently observed in MD simulations of cyano-terminated alkanethiols on gold.[5,6] However, while such an arrangement of dipoles at the monolayer surface may have interesting consequences in interfacial properties, it would affect very little, if at all, the packing and ordering of the alkyl chains. On the other hand, if such an arrangement of molecular dipoles is situated in the bulk, it may certainly affect the packing and ordering in the assembly and, maybe, even the conformation of the individual alkyl chains.

The placement of an $SO_2$ group into an alkyl chain will introduce a certain amount of free volume due to the larger size of the $SO_2$ group (S–O bond length ~1.79 Å compared to the 1.1 Å for the neighboring C–H bonds) and may therefore lead to less closely packed monolayers and possibly less well ordered ones. However, the sulfone group would add much less free volume to the assembly than, for example, an amide group, for which case the formation of H bonds in a plane parallel to the monolayer surface can be assumed. Thus, we thought that the sulfone group,

† Current address: Department of Physics, University of Leeds, Leeds, LS2 9JT United Kingdom.

(1) Evans, S. D.; Urankar, E.; Ulman, A.; Ferris, N. *J. Am. Chem. Soc.* **1991**, *113*, 4121.

(2) Tillman, N.; Ulman, A.; Elman, J. F. *Langmuir* **1990**, *6*, 1512.

(3) Ulman, A.; Willand, C.; Köhler, W.; Robello, D.; Williams, D. J.; Handley, L. *J. Am. Chem. Soc.* **1990**, *112*, 7084.

(4) Shnidman, Y.; Eilers, J. E.; Evans, S. D.; Ulman, A. Manuscript in preparation.

(5) Hautman, J.; Bareman, J. P.; Mar, W.; Klein, M. L. Preprint.

(6) The work presented in this paper was stimulated, in part, by discussions we had with Prof. M. Klein during his visit to Eastman Kodak Co.

0743-7463/91/2407-2700$02.50/0 

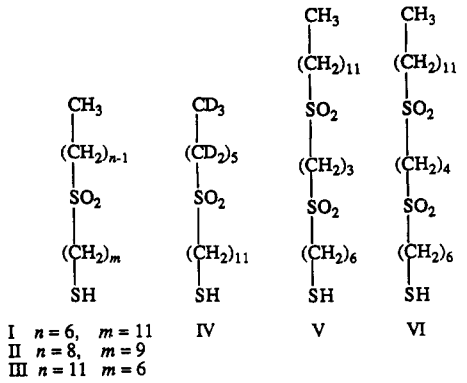


**Figure 2.** Alkanethiols containing one and two sulfone groups.

because of the tetrahedral geometry around the sulfur atom, provides an excellent example for the study of planar intermolecular interactions and their effects on chain packing and ordering. In addition, the position of the $SO_2$ group in the alkyl chain was varied to see how this affected the surface and monolayer properties, while the overall length of the molecules was kept constant.

## Experimental Section

**Materials.** Three sulfones were synthesized in which the positions of the $SO_2$ groups were varied while the total chain length ($C_{17}$) was kept constant (Figure 2). The synthesis is described in detail in the supplementary material. For comparative purposes octadecanethiol (ODT, $CH_3(CH_2)_{17}SH$) monolayers were also studied. This was obtained from Aldrich and used without further purification. Hexadecane was Aldrich Gold Label, and dichloromethane was Kodak. Both were used without further purification.

**Substrate Preparation.** The substrates employed in this study were prepared by the evaporation of gold (99.999%) onto chromium-coated silicon wafers (75 mm × 25 mm). The silicon wafers were cleaned prior to the evaporation using the following procedure: The silicon wafers were rinsed in Millipore water to remove any particulate matter remaining following the scribing of the silicon. They were then ultrasonicated in a mixture of Deconex 12–$H_2O$ (1:10) for 15 min, rinsed, and ultrasonicated with Millipore water. The substrates were then either cleaned by piranha etch[7] or plasma etched using a Harrick plasma cleaner. The silicon substrates were then rinsed and stored in Millipore water until required. The chrome underlayer was deposited from the vapor by resistive heating of a chromium-coated tungsten wire. The deposition rates for the chromium were 1–5 Å/s, and the films had typical thicknesses between 75 and 100 Å. Subsequently, the gold films were evaporated from tungsten holders with deposition rates close to 5 Å/s. The total thicknesses were typically between 1500 and 2000 Å. The pressure in the vacuum chamber was maintained at $7.5 \times 10^{-6}$ Torr during the evaporation, using an Edwards turbomolecular pump. The chamber was vented to atmosphere by backfilling it with filtered nitrogen. The clean gold surfaces were examined by Auger spectroscopy, and only "normal" carbonaceous-type contaminations were found. No chromium was found, indicating that chromium had not diffused from the adhesion layer to the outer surface during the age of the sample (2 weeks). The low-angle X-ray spectrum showed one peak, associated with the (111) face.

Prior to their use the gold substrates were cleaned in the $H_2SO_4$–$H_2O_2$ mixture, at 90 °C, for 5 min. The substrates were rinsed with Millipore water and dried in $N_2$ and their optical constants measured.

**Monolayer Preparation.** Monolayers were formed by immersion, for at least 15 h, in 1 mM solutions of the respective thiol in $CH_2Cl_2$–hexadecane (20:80) or in THF under $N_2$. Monolayers of the disulfones were formed by immersion, for at least 15 h, in 1 mM solutions of the respective thiol in THF under $N_2$.

(7) Substrates were placed in $H_2SO_4/H_2O_2$ (7:1) at 90 °C for 30 min. *Caution! A solution of $H_2O_2$ in $H_2SO_4$ ("piranha" solution) is a very strong oxidant and reacts violently with many organic materials. It should be handled with extreme care.*

**Table I. Contact Angles of Monolayers of I–III**

| molecule | $\theta_{HD}$ | $\theta_{H_2O}$ a | $\theta_{H_2O}$ r |
|---|---|---|---|
| I | 40 | 106 | 97 |
| II | 40 | 108 | 97 |
| III | 41 | 109 | 101 |
| ODT | 45 | 110 | 105 |

**Monolayer Thickness.** The thickness of the monolayers was monitored using a Gaertner L116B ellipsometer equipped with a 632.8-nm helium–neon laser and controlled by an IBM-PC computer. Monolayer thicknesses were determined assuming $n_f = 1.5$, and with the incident and reflected light making a 70° angle to the surface normal. The variation in the measured thickness across the dimensions of any individual sample was ±1 Å.

**Wetting Properties. (a) Captive Drop Technique.** Advancing and receding angle measurements were made by forming a droplet on the end of a square cut hypodermic needle and lowering it until the droplet touched the surface. The advancing contact angle was measured when the volume of the droplet was increased *without increasing the solid–liquid interface area.* Similarly, the receding angle was the minimum angle measured for a droplet as its volume was reduced *without the solid–liquid interface area changing.*

**(b) Free-Standing Droplets.** For the measurements of hexadecane and the various liquids used for the Zisman plots, readings were taken from free-standing droplets. These were made by forming a droplet at the end of a fine-bore capillary tube and lowering it onto the surface. The capillary tube was then removed, and the contact angle of the free-standing droplet was measured. All angles were determined using a Ramè-Hart NRL 100 goniometer.

We note that surface roughness affects both contact angle and contact angle hysteresis.[8-11] Rough surfaces may appear to be more hydrophobic, where in fact, they are just less wettable due to mechanical restrictions on critical line movement (pinning). It is, therefore, important to measure contact angle hysteresis and compare the values to a given standard (e.g., ODT/Au). The presence of large hysteresis in water and hexadecane (HD) contact angles on the standard surface suggests that the gold surfaces are rough and that the evaporation procedure should be reevaluated. Surface roughness for substrates employed in this study is p-v 11.00 Å and the root mean square value is 2.40 Å, for a 130-μm-length scale. Using these surfaces, we measured hysteresis of 5° in the contact angles of water on ODT/Au (Table I). Therefore, our surfaces are not rough on a macroscopic scale. Of course, these substrates are made of small gold crystallites and, hence, are very rough on a microscopic scale. Indeed, roughness studies using X-ray reflectivity gave average p-v values of 20 Å on a length scale of 2800 Å.[12] The use of gold evaporated and annealed on mica,[13] or for this matter on glass microscope slides,[14] provides surfaces with large gold crystals. However, we have found that surfaces of gold evaporated and annealed on mica give monolayers that exhibit large wetting hysteresis, presumably due to pinning.[15] We thus have used gold on silicon as our standard substrates in these studies.

**X-ray Photoelectron Spectra (XPS).** The XPS spectra were obtained on a Hewlett-Packard 5950A photoelectron spectrometer, which has a monochromatic Al Kα X-ray source (1486.6 eV). The use of a monochromatic source minimizes sample radiation damage. The pressure in the spectrometer was typically $2 \times 10^{-9}$ Torr. Angle-dependent measurements were made using a Surface Science Laboratory Model 259 angular rotation probe.

(8) Dette, R. H.; Johnson, R. E. *Adv. Chem. Ser.* **1964**, *43*, 136.
(9) Joanny, J. F.; de Gennes, P. G. *J. Chem. Phys.* **1984**, *81*, 552.
(10) de Gennes, P. G. *Rev. Mod. Phys.* **1985**, *57*, 827.
(11) Ray, B. R.; Bartell, F. E. *J. Colloid Sci.* **1953**, *8*, 214.
(12) Pershan, P. S.; Tidswell, I. Unpublished results.
(13) Chidsy, C. E. D.; Loiacono, D. N.; Sleator, T.; Nakahara, S. *Surf. Sci.* **1988**, *200*, 45.
(14) Rubinstein, I. Private communication.
(15) Evans, S. D.; Ulman, A. Unpublished results.

The magnification of the four-element electron lens was altered from −5.0 to −2.3 to reduce the electron acceptance solid angle of the electron lens from a 3.5° cone to a 2.8° half-angle cone.

**Infrared Measurements.** The infrared spectra of samples in KBr pressed pellets and in solution were measured with a Perkin-Elmer 1430 spectrometer at a resolution of ±1 $cm^{-1}$. Grazing-angle (reflection–absorption) FTIR spectra were measured with an IBM IR44 spectrometer at a grazing angle of 76°. Band frequencies are accurate to ±2 $cm^{-1}$.

## Results and Discussion

**Ellipsometry and Wetting.** All three compounds (I–III) yielded monolayers with thicknesses of 19 ± 2 Å, as determined by ellipsometry. From simple Corey–Pauling–Koltun (CPK) model measurements, this implies an average molecular tilt of ~40 ± 8° to the surface normal, for complete monolayers in which the alkyl chains are all-trans. The wetting properties for water and hexadecane are given in Table I, and it appears that the free energy of the surface *increases* as the length of the alkyl chain *above* the $SO_2$ groups is *decreased*. Such an increase in the surface free energy may be associated with either a lower packing density of methyl groups at the surface or with increasing disorder as the chain length above the $SO_2$ group is reduced. Another possible contribution to the observed decrease in surface free energy is due to the position of the dipole associated with the $SO_2$ group relative to the surface. However, we believe that the latter is not the major contribution since we have also observed this phenomenon in other systems,[1] in which there was not sulfone group.[16] From Zisman plots[17] it is found that all give critical surface tensions close to 21 mN $m^{-1}$ (using a homologous series of *n*-alkanes), which is higher than the 19 mN $m^{-1}$ expected for typical $CH_3$-terminated monolayers.[18] We will discuss these results further, but first we wish to introduce the FTIR and XPS results.

**Fourier Transform Infrared Reflection Absorption Spectroscopy.** The frequencies, shapes, and intensities of the infrared C–H stretching bands provide information on the orientation, conformation, and packing of the hydrocarbon chain in the monolayers. In the present case, however, an analysis of these bands is made somewhat more complicated by the $SO_2$ groups which can be expected to perturb the frequencies and intensities of the C–H stretching vibrations of the methylene and methyl groups that are in the immediate vicinity. The spectra of model compounds indicate that the frequencies of the $d^-$ ($\nu_{as}(CH_2)$) and $d^+$ ($\nu_s(CH_2)$) modes of a $CH_2$ next to an $SO_2$ group are increased by roughly 30 $cm^{-1}$. The C–H stretching mode of the next nearest $CH_2$ is no doubt also affected, but probably much less. As the length of the $(CH_2)_m$ segments increases (Figure 2), the peak frequencies of the $d^-$ and $d^+$ bands move toward their unperturbed values. The last vestige of the $SO_2$ group is manifest in an asymmetric band shape. The methylene groups nearest the $SO_2$ group(s) contribute intensity to the high-frequency side. Some asymmetry in the $d^-$ bands of monolayers I–III may be seen in Figure 3. In contrast, the $d^-$ band of ODT, also shown in this figure, is nearly symmetric. The $d^+$ band is probably affected in a similar way.

The $SO_2$ group also acts to vibrationally decouple the chains on either side. As a result, a given methylene C–H stretching band, $d^-$ or $d^+$, consists of superimposed bands from two or more decoupled polymethylene segments. In principle, a band associated with any given segment can be isolated by deuterating the other segments. (See below).

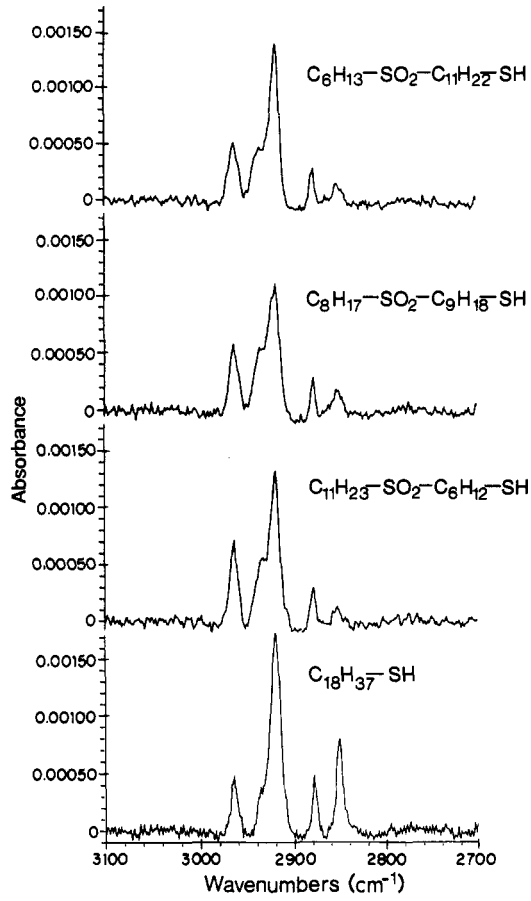


**Figure 3.** FTIR spectra of monolayers of I–III and of ODT in the C–H stretching vibrations region.

Several interesting features emerge from the reflection–absorption FTIR data. In the high-frequency region (Table II) associated with the $CH_2$ and $CH_3$ stretches, the asymmetric stretches ($d^-$ and $r^-$) are observed to be much more intense than the symmetric stretches ($d^+$ and $r^+$, Figure 3). The value of the integrated intensity ratio, $R = I(d^-)/I(d^+)$, is essentially the same for the three monolayers of I–III (~20 ± 10, Table III). This indicates that these monolayers are isostructural and that their constituent chains are preferentially oriented in a way that may be described as "anisotropic." In contrast, we note that $R$ is near 2.0 for randomly oriented samples of polycrystalline *n*-alkanes.[19] The factor of 10 difference between these values is a clear indication that the sulfone-substituted chains are tilted and that the tilt is predominately in a direction perpendicular to the skeletal plane on the chains. From the ellipsometric value of ~40° for the overall tilt in combination with the observed value of $R$ for the monolayer and polycrystalline samples, we find that the average tilt perpendicular to the plane of the skeleton is around 35° and in the plane 10 ± 3°.

Tilt of the kind just described indicates that the chain packing is not orthorhombic. In the case of orthorhombic packing, which is the type of packing normally found in crystalline monolayers, there are two chains in the unit subcell and their skeletal planes are very close to being mutually perpendicular. The effect of chain tilt is therefore the same for both the $d^-$ and $d^+$ bands, so that $R$ assumes a value that is the same as that for a random polycrystalline sample, that is, 2.0. For example, for

(16) Tillman, N.; Ulman, A.; Schildkraut, J. S.; Penner, T. L. *J. Am. Chem. Soc.* **1988**, *110*, 6136.
(17) Zisman, W. A. *Adv. Chem. Ser.* **1964**, *43*, 1.
(18) Bain, C. D.; Troughton, E. B.; Tao, Y.-T.; Evall, J.; Whitesides, G. M.; Nuzzo, R. G. *J. Am. Chem. Soc.* **1989**, *111*, 321.
(19) Snyder, R. G. *J. Chem. Phys.* **1965**, *42*, 1744.

**Table II. IR Peak Assignments for Monolayers of I–VI**

| peak | KBr | $CH_2Cl_2$ | I | II | III | ODT | IV | V | VI |
|---|---|---|---|---|---|---|---|---|---|
| $CH_3\ \nu_{as}(r^-)$ | *a* | *a* | 2963 | 2963 | 2963 | 2965 | | 2963 | 2963 |
| $CH_3\ \nu_{as}(r^-)$ | 2954 | 2955 | *b* | *b* | *b* | *b* | | *b* | *b* |
| $CH_3\ \nu_s(FR)(r^+)$ | *a* | *a* | 2936 | 2936 | 2936 | 2936 | | 2936 | 2936 |
| $CH_2\ \nu_{as}(d^-)$ | 2919 | 2929 | 2918 | 2919 | 2919 | 2919 | 2919 | 2920 | 2919 |
| $CH_3\ \nu_s(r^+)$ | *a* | 2871 | 2878 | 2878 | 2878 | 2878 | | 2879 | 2878 |
| $CH_2\ \nu_s(d^+)$ | 2847 | 2857 | 2852 | 2852 | 2852 | 2852 | 2849 | 2851 | 2853 |
| CD | | | | | | | | 2220 | |
| CD | | | | | | | | 2074 | |
| $SO_2\ \nu_{as}$ | 1328 | *a* | 1327 | 1327 | 1326 | | 1317 | 1322[c] | 1329 |
| $SO_2\ \nu_s$ | 1127 | 1131 | *b* | *b* | *b* | | 1143 | *b* | *b* |
| CH(w) | *d* | | 1275 | 1275 | 1274 | | 1278 | | |
| CH(w) | *d* | | 1259 | | 1259 | | 1261 | 1265 | |
| CH(w) | *d* | | | 1251 | | | | 1249 | |
| CH(w) | *d* | | 1236 | | 1236 | | 1237 | | 1234 |
| | | | | | | | | 1212 | 1215 |

[a] Not resolvable in the KBr or $CH_2Cl_2$ spectra. [b] Could not be detected in the monolayer spectra. [c] The monlayer and KBr peaks were at the same position. [d] The wagging modes in the KBr spectra were invariably very close to those found in the monolayer spectra, and the corresponding solution spectra were not resolvable.

**Table III. Area under CH Peaks**

| peak | I | II | III | ODT |
|---|---|---|---|---|
| $CH_3\ \nu_{as}(r^-)$ | 0.0064 | 0.0064 | 0.0064 | 0.0039 |
| $CH_2\ \nu_{as}$, $CH_3\ \nu_s$ ($r^+$, $d^-$) | 0.0232 | 0.0214 | 0.0215 | 0.0261 |
| $CH_3\ \nu_s(r^+)$ | 0.0013 | 0.0007 | 0.0008 | 0.0025 |
| $CH_2\ \nu_s(d^+)$ | 0.0016 | 0.0019 | 0.0006 | 0.0075 |
| total | 0.0325 | 0.0304 | 0.0297 | 0.0400 |

**Table IV. Measured Full Width at Half-Maximum of the $r^-$ and $d^-$ Bands**

| | fwhm, $cm^{-1}$ | |
|---|---|---|
| monolayer | $r^-$ | $d^-$ |
| I | 13 | 13 |
| II | 12 | 18 |
| III | 10 | 13 |
| ODT | 9 | 13 |
| IV | | 11.4 |
| V | 8.4 | 13 |
| VI | 6.4 | 11 |

straight alkanethiol monolayers on gold, $R$ is typically around 2.2.[20] Indeed, for the ODT monolayers in this study we find $R = 2.2$.

Chain packing in the alkyl sulfone monolayers I–III is probably triclinic. The triclinic subcell contains just one chain per subcell, so that the skeletal planes of all the chains are parallel. To verify triclinic packing, we have attempted to determine the shape of the $CH_2$ scissors mode at 1460 $cm^{-1}$ to see if it consists of one component (triclinic) or two components (orthorhombic). Unfortunately, we were not successful because the $CH_2$ scissors mode has the same symmetry as the $d^+$ mode, so that its intensity is much reduced in the monolayer spectrum.

The monolayer bands in this region have frequencies that are closer to those found in the KBr spectra than those in solution, suggesting that the monolayers are more "solidlike" than "liquidlike". In fact we found little spectroscopic evidence of any kind of a significant degree of conformational disorder. Conformational disorder is manifest mainly through a shift upward in the frequency of the $d^-$ band. For example, in going from a crystalline to an amorphous state, the shift is about 8 $cm^{-1}$.[21] The frequency we observe for the $d^-$ band is 2919 $cm^{-1}$, which is within $\pm 1$ $cm^{-1}$ of that found for alkyl chains in crystalline monolayers or in Langmuir–Blodgett (LB) multilayers. Our monolayers are therefore highly crystalline.

We have used the width of the C–H stretching bands as a measure of the tightness of the chain packing in the monolayer. Chain packing in the crystalline state may be described as loose or tight even in the absence of disorder. Loose chain packing covers both the static case, which involves steric mismatch, or the dynamic case, which involves large-amplitude motion. Loose chain packing in a system of all-trans chains results in an increase in the width of the $d^-$ band.[22] At the chain end, looseness is reflected in an increase in the width of the $r^-$ band.[23] We will use the fwhm (full width at half-maximum) as a measure of bandwidth, $\Delta\nu_{1/2}$.

The observed values of the fwhm of the methylene asymmetric C–H stretching band, $\Delta\nu_{1/2}$ ($d^-$), for the sulfone-containing alkanethiol monolayers are generally in the range 11–13 $cm^{-1}$ (Table IV); for ODT a value of 13 $cm^{-1}$ is found. This indicates that the chain packing for the monolayers is well ordered since a comparable width, 11 $cm^{-1}$, is found for $d^-$ in the case of crystalline $n$-$C_{20}H_{42}$, which is a tightly packed. An example of loosely packed $n$-alkane chains is found in $n$-alkane urea–clathrates, in which at room temperature the chains exhibit a high degree of librational/rotational motion that leads to a broad $d^-$ band whose width is about 18 $cm^{-1}$.[22]

Monolayers of sample II show an anomalously high $d^-$ bandwidth of 18 $cm^{-1}$. The high value may be related to the fact that the $SO_2$ group in this case is near the center of the chain so that the longest segment in this monolayer is shorter than the longest segment found in any other monolayer. The inferred correlation that longer chains lead to tighter packing is supported by measurements on partially deuterated monolayer IV to be described below.

Monolayer I consists of chains in which $C_{11}H_{22}$ and $C_6H_{13}$ chain segments are separated by an $SO_2$ group. We have found that the packing in the $C_{11}H_{22}$ segment is nearly as tight as that found in a crystalline $n$-alkane, while in contrast the $C_6H_{13}$ segment is loosely packed. These findings follow from two kinds of measurements. The infrared spectrum of the partially deuterated monolayers, $CD_3$–$(CD_2)_5$–$SO_2$–$(CH_2)_{11}$–S/Au, shows the width of the $d^-$ of the $(CH_2)_{11}$ segment to be 11 $cm^{-1}$. Thus, tight packing is indicated. Evidence that the packing of the shorter chain is not as tight is inferred from the width of the $r^-$ band (Table IV). For monolayers I, II, and III,

(20) Porter, M. D.; Bright, T. B.; Allara, D. L.; Chidsey, C. F. D. *J. Am. Chem. Soc.* **1987**, *109*, 3559.
(21) Snyder, R. G.; Strauss, H. L.; Elliger, C. A. *J. Phys. Chem.* **1982**, *86*, 5145.
(22) Wood, K. A.; Snyder, R. G.; Strauss, H. L. *J. Chem. Phys.* **1989**, *91*, 5255.
(23) MacPhail, R. A.; Snyder, R. G.; Strauss, H. L. *J. Chem. Phys.* **1982**, *77*, 1118.

whose upper segments have lengths $C_6$, $C_8$, and $C_{11}$, respectively, $\Delta\nu_{1/2}$ ($r^-$) is observed to be 13, 12, and 10 $cm^{-1}$. This clearly indicates a trend then toward tighter packing as polymethylene segments become longer, a trend that is consistent with that found from the wetting data. In keeping with these results we note, for ODT, $\Delta\nu_{1/2}$ ($r^-$) is less than 10 $cm^{-1}$.

The integrated intensities of the C–H bands provide additional data on tilt and disorder in the monolayers. For an "ideal" monolayer, in which the alkyl chains are all-trans and are perpendicular to the plane of the film, only the $CH_3$ stretches should be observed in the absorption spectra, in a grazing incident experiment.[24] Tilt and/or disorder results in the $CH_2$ vibrations contributing intensity. The relative intensities of the stretching bands can thus be used to indicate tilt or disorder for the alkyl chains. Table III shows that the "total integrated C–H intensity" *increases* as the length of the alkyl chain above the $SO_2$ group *decreases*. It is, therefore, concluded that *the order within the monolayers is higher for molecules with longer alkyl chains above the bulky polar group.* This result agrees with the IR bandwidth and wetting results. The intensities of the asymmetric vibrations are only slightly dependent on the $SO_2$ position, in contrast to the situation for the symmetric stretching vibrations. This may be seen in Table III for monolayers of I and III. The "total" C–H intensity between 3100 and 2700 $cm^{-1}$ gives I/III = 1.094, while for individual stretches I/III = 1 ($r^-$), 1.0790 ($d^-$, FR, 1.625 ($r^+$), and finally 2.6667 ($d^+$). This increase in the symmetric stretch intensity suggests a change in the tilt angle in the plane of the carbon skeleton. Additional evidence for this is the appearance of the sulfone symmetric stretch at ~1126 $cm^{-1}$ for some monolayers of I and at 1146 $cm^{-1}$ for monolayers of IV.

The methylene wagging bands that appear between the $SO_2$ symmetric and asymmetric bands have slightly different frequencies for different monolayers. These peaks appear in the KBr bulk spectra at frequencies only slightly shifted from those for the monolayers (Figure 4). The peak intensities of these bands *decrease* as the length of the alkyl chain above the $SO_2$ is *increased*. This may reflect a sensitivity to the molecular environment and in principle provide information about the order/crystallinity within these monolayers. Since a similar wagging distribution is found in the partially deuterated monolayers, it seems reasonable to assume that these vibrations have their origin in the portion of the alkyl chain between the gold surface and the $SO_2$ group, indicating that the alkyl chains below the $SO_2$ group are not disordered. This would also explain why the intensity of the wagging vibrations decreases as the length of the alkyl chain below the $SO_2$ group is reduced. Thus, the presence of these peaks does not allow us to reach any conclusions on the order within these monolayers above the $SO_2$ group.

The spectrum of the partially perdeuterated monolayer IV in the region between 3100 and 2700 $cm^{-1}$ is similar to that for undeuterated monolayers shown in Figure 3, except, of course, that there are no $CH_3$ bands. In the C–D stretching region, only two intense bands are observed, at 2220 and 2074 $cm^{-1}$ (Figure 5). The C–D stretching bands of the $C_6D_{13}$ segment of the partially deuterated monolayer IV are not, unfortunately, easily interpretable diagnostic probes. The significant differences between the spectrum of $C_6D_{13}$ and the spectra reported for ordered, long perdeuterated alkyl chains are symptomatic of this.[25]

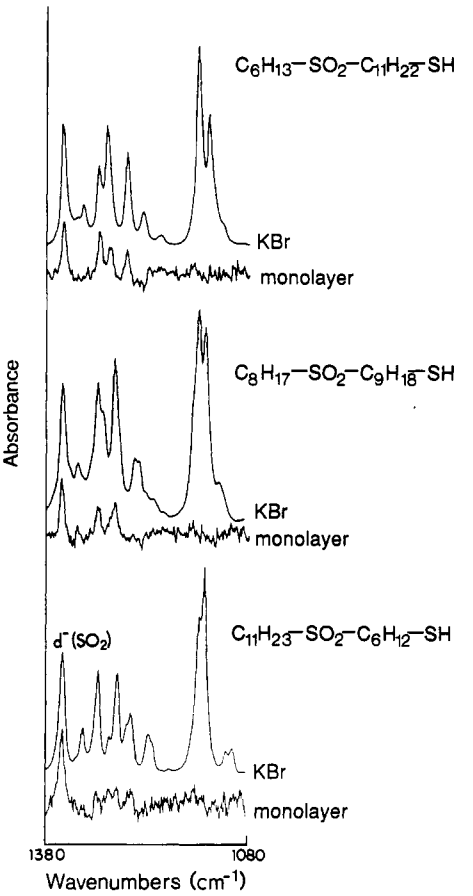


**Figure 4.** FTIR spectra of I–III in KBr and in monolayers on gold in the 1380–1080-$cm^{-1}$ region.

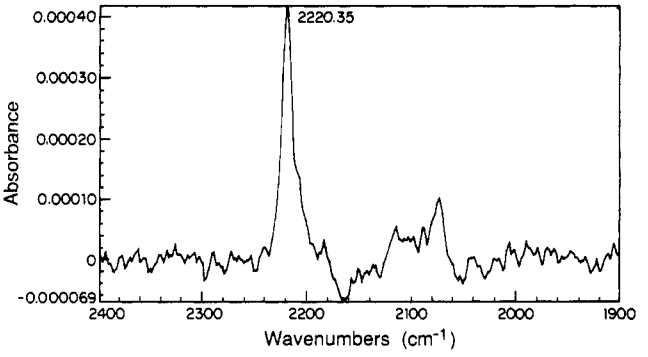


**Figure 5.** FTIR spectrum of a monolayer of $C_6D_{13}-SO_2-(CH_2)_{11}-SH$ on gold in the C–D stretching vibrations region.

These differences are largely attributable to the difference in the lengths of the segments rather than to differences in disorder. If the chain is sufficiently short, the effect on frequencies and intensities of C–H or C–D stretching bands by an $SO_2$ group, or even by the methyl group,[26] can be quite large relative to that from disorder. In addition, the condition of near in-phase motion (large $k$ vector) that drastically simplifies the spectra of long ordered chains is relaxed for short chains. In the present case, the frequencies of the $d^-$ and $d^+$ bands of the $C_6D_{13}$ segment appear to be shifted upward by the $SO_2$ group from their expected values of around 2200 and 2095 $cm^{-1}$ [25] to around 2220 and 2110 $cm^{-1}$, respectively. The $r^-$ and $r^+$ bands of the $CD_3$ group are still relatively unaffected (2220 and 2070 $cm^{-1}$, respectively). The most intense band in the

(24) Blanke, J. F.; Vincent, S. E.; Overend, J. J. *Spectrochim. Acta, Part A* **1976**, *32*, 163.

(25) Levin, I. W. *Advances in Infrared and Raman Spectroscopy*; Wiley-Heyden: New York, 1984; Vol II.

(26) Snyder, R. G.; Scherer, J. R. *J. Chem. Phys.* **1979**, *71*, 3221.

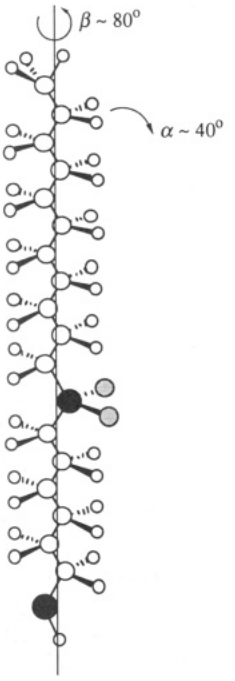


**Figure 6.** A schematic view of a $C_6H_{13}$–$SO_2$–$(CH_2)_{11}$–SH molecule with the proposed tilt and rotation angles.

C–D spectrum, near 2220 $cm^{-1}$, is therefore likely to be a superposition of the $r^-$ and $d^-$ bands. This assignment conflicts with that of Dote and Mowery who assigned the 2220-$cm^{-1}$ band to $r^-$ alone.[27]

In Figure 4, in the region between 1350 and 1050 $cm^{-1}$, the strong band near 1326 $cm^{-1}$ is attributed to the S–O asymmetric stretching mode of the $SO_2$ group. The S–O symmetric stretching mode, which is expected to occur close to 1127 $cm^{-1}$, is not observable (it was just discernible in some of the spectra of monolayers of I and slightly more so in those of IV). KBr spectra of the bulk and $CH_2Cl_2$ solution spectra show that the intensity of the symmetric $SO_2$ band is large, comparable to that of the asymmetric $SO_2$ vibration. The absence of the symmetric $SO_2$ band in the monolayer spectrum is due to the surface selection rule. This means that the transition dipole of the symmetric $SO_2$ mode is parallel to the monolayer plane. This, taken together with the results from the high-frequency region, yields specific details of the molecular conformation in the monolayer: The $\nu_s(SO_2)$ and $d^+$ lie in approximately the same plane, this plane is parallel to the substrate surface, and this implies that there is little, if any, twist about the $C(H_2)$–$S(O_2)$ bonds. Ellipsometric measurements suggest that the molecules exhibit an *average* molecular tilt of $\sim 40 \pm 8°$ to the surface normal. For the transition moment of the symmetric C–H and S–O stretching bands to remain in the plane of the film, the molecules must tilt in one dimension. The structure proposed shown in Figure 6 is consistent with our interpretation of the observed FTIR and ellipsometric data. In this figure, $\alpha$ is the tilt angle relative to the surface normal and $\beta$ is the rotation about the molecular axis. From the experimental data we find $\alpha \approx 40°$ and $\beta \approx 80°$.[28,29]

**Angle-Resolved X-ray Photoelectron Spectroscopy.** Angle-resolved XPS measurements were made on two of the monolayer samples, I and III, in order to follow the change in concentration of various elements with analysis depth. The concentration of each element as a function of electron takeoff angle for sample I is presented in Table V. As expected, the concentration of both types of sulfur decreases while the concentration of gold increases for greater electron takeoff angles. There is one abnormality in the results from Table V. The oxygen to sulfur ratio is between 1.5:1 and 1.8:1 for the sulfone group, for all angles as expected, except for 10° where the ratio changes drastically to 0.4:1. The difference in the inelastic mean free path (IMFP) for the S 2p and the O 1s electrons could account for a small discripancy (~20%) but not one of this magnitude. A possible explanation for this discrepancy is that the actual IMFP for O 1s electrons may be much smaller than predicted theoretically. Thus, at very low takeoff angles very few O 1s electrons can be detected.

**Table V. Atomic Percent versus Takeoff Angle for a Monolayer of I**

| | atomic percent | | | | |
|---|---|---|---|---|---|
| element | 10° | 20° | 30° | 38° | 78° |
| carbon | 66.2 | 54.6 | 44.9 | 42.9 | 36.4 |
| oxygen | 7.1 | 5.8 | 5.8 | 5.2 | 5.0 |
| sulfur ($SO_2$) | 17.2 | 4.0 | 3.8 | 3.2 | 2.7 |
| sulfur (S/Au) | 4.2 | 1.4 | 1.3 | 1.3 | 1.3 |
| gold | 5.4 | 34.1 | 44.5 | 47.4 | 54.6 |

One very important feature noticed during the data analysis was the shape of the sulfur 2p peak. A high-resolution scan of the sulfur 2p region should resolve the $2p_{1/2}$ and the $2p_{3/2}$ doublet, which should have an area ratio of 1 to 2. The peaks due to the $SO_2$ sulfur and the thiol sulfur should also be resolved, with the $SO_2$ sulfur occurring at about 5 eV higher than the thiol sulfur (chemisorption of alkanethiols on gold gives the gold($\delta^+$) thiolate ($RS^{\delta-}$) species, thereby making it easier to remove electrons from the thiolate, causing the sulfur peaks to shift to lower binding energy). Since the oxygen is an electron-withdrawing group, the peaks due to the $SO_2$ sulfur are shifted to a higher binding energy. A high-resolution scan of the sulfur 2p region for monolayers I and III is presented in Figure 7. The two types of sulfur are easily resolved for III (Figure 7a), and the ratio between the $2p_{1/2}$ and the $2p_{3/2}$ doublet is 1:2. Figure 7b is representative of the spectra obtained for all of the takeoff angles for sample I. Notice that while the two sulfur doublets are resolved, the lower binding energy doublet does not have the characteristic 1:2 ratio. This peak, in fact, consists of two sets of doublets as the peak fitting routine shows. The lower energy doublet belongs to the thiol sulfur while the higher energy doublet is due to $SO_2$ sulfur that has been reduced. The areas of reduced $SO_2$ sulfur peaks were added to the area of the highest binding energy sulfur peak to determine the total amount of $SO_2$ sulfur. Reduction of the $SO_2$ sulfur was later confirmed when a sample was analyzed for a short time period and then analyzed overnight. Evidence of the developing higher binding energy doublet is clearly shown after the overnight analysis.[30] Due to the fact that reduction of the $SO_2$ sulfur occurs after long analysis times, only the sulfur 2p high-resolution spectrum was acquired at each angle for sample III. Two possible causes for the $SO_2$ reduction are effects from X-ray exposure and effects from secondary electrons originating from the gold substrate.

The results for samples I and III plotted as a function of takeoff angle vs the ratio of $SO_2$ sulfur to thiol sulfur

(27) Dote, J. L.; Mowery, R. L. *J. Phys. Chem.* **1988**, *92*, 1571.
(28) (a) Allara, D. L.; Swalen, J. D. *J. Phys. Chem.* **1982**, *86*, 2700. (b) Allara, D. L.; Nuzzo, R. G. *Langmuir* **1985**, *1*, 52.
(29) (a) Nuzzo, R. G.; Fusco, F. A.; Allara, D. L. *J. Am. Chem. Soc.* **1987**, *109*, 2358. (b) Allara, D. L.; Baca, A.; Pryde, C. A. *Macromolecules* **1978**, *11*, 1215.

(30) Further support for the reduction of the sulfone has also been seen in SERS experiments; see ref 1.

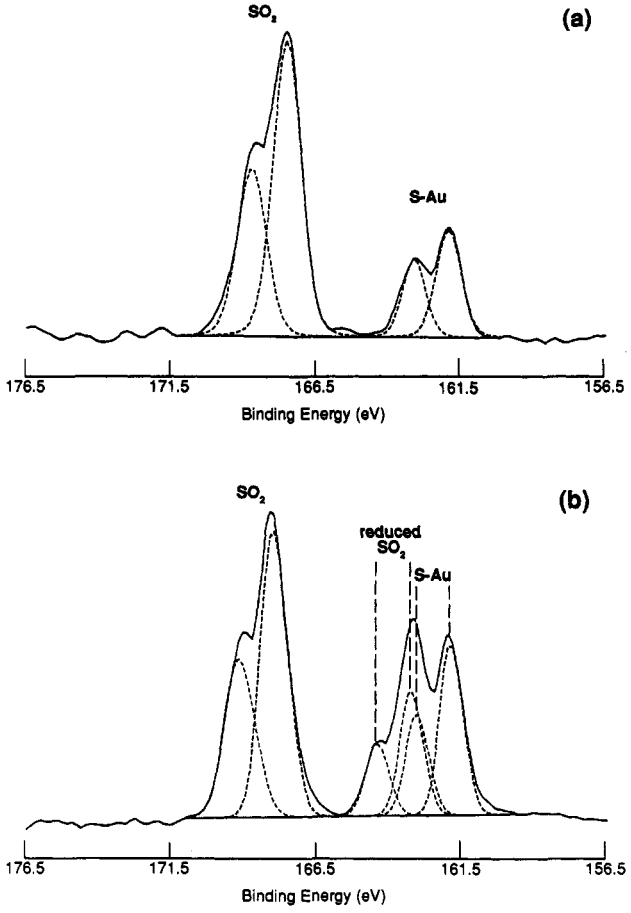


**Figure 7.** High-resolution XPS spectra of the $S_{2p}$ region for a monolayer of III (a) and I (b) taken at an electron takeoff angle of 20°. The analysis times were ~2 h for sample III and ~15 h for sample I.

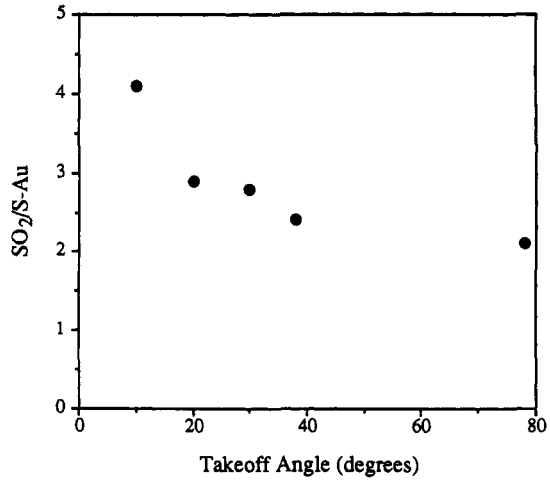


**Figure 8.** Takeoff angle vs $SO_2$:S/Au for a monolayer of I.

($SO_2$:S/Au) are shown in Figures 8 and 9, respectively. Qualitatively, the shapes of both curves are similar. With increasing takeoff angle, the ratio of $SO_2$ to S/Au should decrease as the analysis depth increases and the $SO_2$ sulfur becomes less predominant. In both graphs there is a break in the curve occurring at 30° in sample I and 38° in sample III. Notwithstanding the limited data above 40°, these breaks are deemed real and not artifacts. As the takeoff angle is varied, the effective analysis depth also changes. Thus, a depth should be reached that corresponds to an optimum escape depth for the electrons from a particular atom. If we assume a value of 26 Å for the IMFP of 1300-eV electrons in an organic matrix, the data suggest that

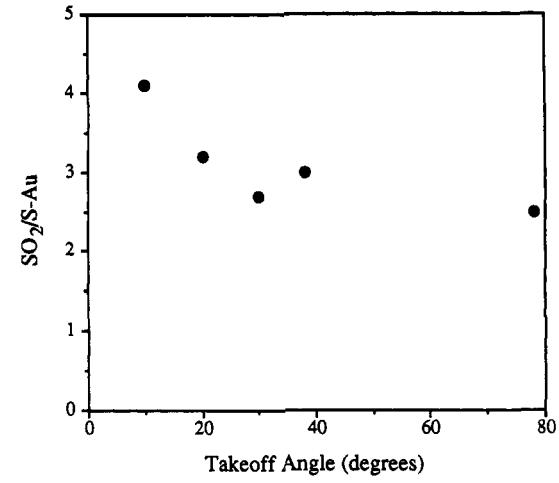


**Figure 9.** Takeoff angle vs $SO_2$:S/Au for a monolayer of III.

the $SO_2$ sulfur in sample I is 3 Å closer to the surface than the $SO_2$ sulfur in sample III.[31] If the molecules are in an all-trans arrangement and the alkyl chains are oriented perpendicular to the surface, we estimate from space-filling models the $SO_2$ sulfur to be at 7.75 and 14 Å from the surface in samples I and III, respectively. If the chains exhibit on the average a tilt of 40°, as indicated from both ellipsometry and FTIR data, then the difference in the optimum escape depth for the two molecules is found to be 3 Å from the experiment and 5 Å from the space-filling model.

Analysis of the angle-dependent data can provide an estimate of the thickness of the overlayer and indicate if the overlayer is continuous. Our method of analysis is similar to that reported previously.[32] An equation for the angle-dependent ratio of the overlayer to the substrate was developed by Fadley[33] where $\tau$ = effective overlayer

$$R_{\text{overlayer/substrate}} = K[\exp(\tau/\sin\theta) - 1] \qquad (1)$$

thickness, $\theta$ = electron takeoff angle, and $K$ is a constant. $K$ is dependent on several instrument parameters and the atom density. For simplicity, $K$ was assumed to have a value of 1.0. The concentration of a particular atom in the overlayer and of a different atom in the substrate must be known for the calculation. Since only sulfur was measured in sample III, the above calculation will be applied to sample I only.

A plot of $1/\sin\theta$ vs $\ln [R_{(\text{overlayer/substrate})}/K + 1]$ should give a straight line of slope $\tau$ passing through the origin. Figure 10 shows the plot obtained for sample I, for the thiol S and the gold. The excellent correlation achieved to a straight line fit suggests that the monolayer is continuous. If it had been patchy, the data at low $\theta$ values would deviate from the straight line. The overlayer thickness can be calculated from the slope of the straight line by using the following equation

$$\tau = t/\Lambda_{\text{overlayer}} \qquad (2)$$

where $\tau$ is the slope, $t$ is the actual overlayer thickness, and $\Lambda$ is the electron inelastic mean free path. With a value of 26 Å for $\Lambda$, the overlayer thickness is 0.72 Å. However, this is only the thickness of the thiol sulfur at the gold interface and not the entire overlayer. The value

(31) Seah, M. P.; Dench, W. A. *SIA, Surf. Interface Anal.* **1979**, *1*, 2.
(32) Gerenser, L. J.; Pochan, J. M.; Mason, M. G.; Elman, J. F. *Langmuir* **1985**, *1*, 305.
(33) Fadley, C. S. *Prog. Solid State Chem.* **1976**, *2*, 265.

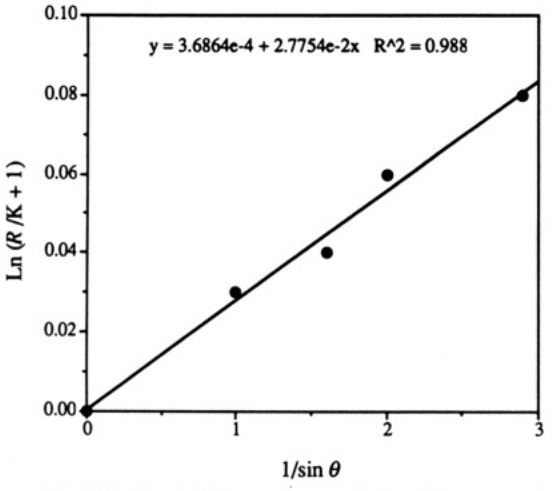


**Figure 10.** $1/\sin\theta$ vs $\ln [R_{overlayer/substrate}/K + 1]$ for a monolayer of I using the thiol sulfur.

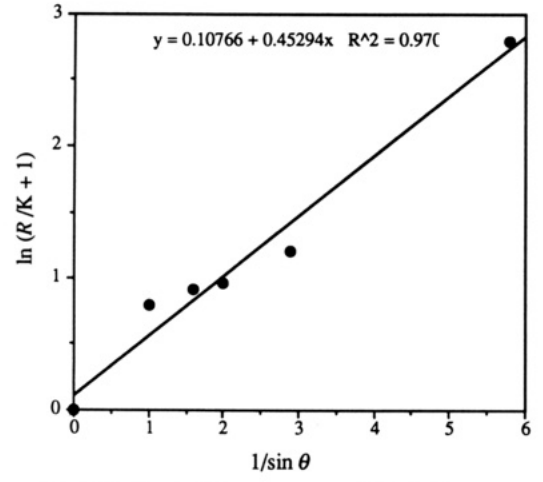


**Figure 11.** $1/\sin\theta$ vs $\ln [R_{overlayer/substrate}/K + 1]$ for a monolayer of I using the $SO_2$ sulfur.

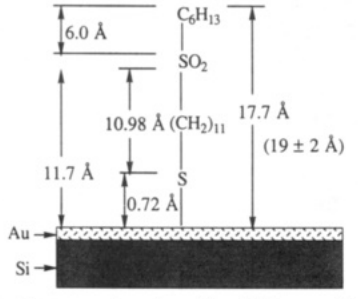


**Figure 12.** A diagram showing the thickness for $C_6H_{13}$–$SO_2$–$(CH_2)_{11}$–SH monolayer as determined by XPS. The number in parentheses is the thickness estimated by ellipsometry.

obtained is in reasonable agreement with the covalent radius for sulfur, which is 1.09 Å.

Similar calculations can also be performed for the $SO_2$ sulfur. The plot obtained is shown in Figure 11. Although the correlation is not as good as the previous graph, the data is reasonable. The overlayer thickness calculated from the slope is 11.7 Å. This does not take into account the six-carbon chain above the $SO_2$ group. The thickness of the lower ($C_{11}$) hydrocarbon chain can thus be estimated to be 11 Å (11.7–0.72 Å). Using the value of 1 Å/chain unit found above, one can then calculate what the thickness of the six-carbon chain should be (6.0 Å, see Figure 12). A thickness of 17.7 Å is obtained for the entire overlayer. This compares favorably to the 19 ± 2 Å estimated from ellipsometry. Unfortunately, the same calculations could not be performed on sample III since gold was not analyzed at each takeoff angle due to the desire for short exposure times.

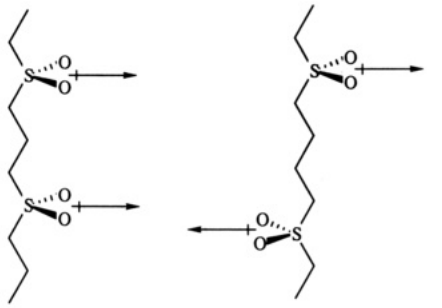

**Figure 13.** A scheme showing two sulfone groups in an alkyl chain.

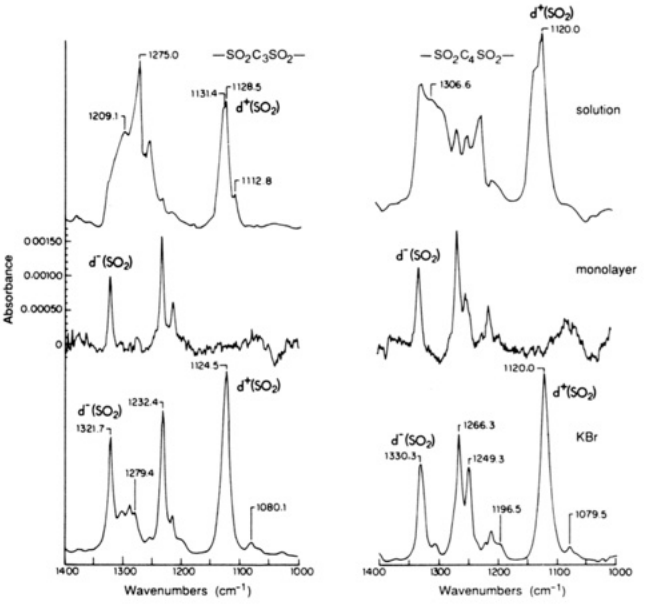


**Figure 14.** FTIR spectra of V and VI in $CH_2Cl_2$ solution, in KBr and in monolayers on gold in the 1300–1000-$cm^{-1}$ region.

**Monolayers Containing Two Sulfone Groups.** The effect of adding a second sulfone group into the chain was investigated. One particular aim was to see if the order within the monolayer was dependent on whether the dipoles of the sulfone groups were parallel or antiparallel. For this purpose, two new sulfones were made (Figure 13, synthesis described in supplementary material). The distance between the sulfone groups was kept small to enhance the dipole–dipole interactions. Disorder in the monolayer might arise either from *intramolecular* electrostatic interactions (repulsive forces) between the sulfone groups or from *intermolecular* interactions between sulfone groups of neighboring chains. Both disulfones were found to be less soluble than the monosulfones I–III, and this is attributed to the electrostatic interactions found in these materials. Both disulfones produced monolayers with critical surface tensions between 20 and 21 mN $m^{-1}$ and in this respect were similar to monosulfones I–III. Large differences, however, were found in the FTIR reflection absorption spectra for molecules of V and VI (parallel and antiparallel dipoles, respectively) in the 1400–1000-$cm^{-1}$ region (Figure 14). The spectra in the C–H stretch region were similar to those for monolayers of I–III, with the exception that the $d^+$ bands were still further reduced in intensity so that they hardly were distinguishable from the background noise. Values of $\Delta\nu_{1/2}$ ($r^-$) are found to be less than 10 $cm^{-1}$ for monolayers of V and VI, and this suggests very tight chain packing. We

must note, however, that the correlation between $\Delta\nu_{1/2}$ ($r^-$) and chain-packing looseness is valid only if the monolayer chains have similar tilt angles. (This requirement which seems fulfilled for monolayers I–III is necessary because the $r^-$ band consists of two bands ($r_a^-$ and $r_b^-$) separated by about 8 $cm^{-1}$ whose transition dipoles are mutually orthogonal.[23] The band shape of $r^-$ is determined in part by the relative intensities of $r_a$ and $r_b$, the relative intensities being dependent on the tilt angle.) The bandwidths of the $d^-$ and $r^-$ bands (Table IV) both indicate that monolayer VI, whose intrachain $SO_2$ groups are antiparallel, is packed more tightly than V.

In the sulfone region, 1400–1000 $cm^{-1}$, the differences are more dramatic. The sulfone asymmetric S–O stretching band has twice the intensity of that for monolayers I–III. This is, of course, expected if the second sulfone group introduced has the same orientation as the first one. The sulfone symmetric stretch bands for monolayers of V and VI were not observable at all (Figure 14), again as is the case of monolayers I–IV. For monolayer V, in which the sulfone groups are parallel, their asymmetric stretch band position is shifted 5 $cm^{-1}$ to lower frequency, 1322 $cm^{-1}$ (for both KBr and monolayers). In contrast, the asymmetric stretch is shifted by approximately 3 $cm^{-1}$ to higher frequencies, if the sulfone groups are antiparallel, so that there is an 8-$cm^{-1}$ difference in the position of the asymmetric sulfone stretch for the two materials. The shift to lower frequency for monolayer V may be indicative of induced disorder.

Figure 13 shows a schematic of the configurations expected in the sulfone portion of the molecules. Assuming that the dipoles lie in the same plane, we find to a first-order approximation that simple electrostatics gives the energy contribution of the dipolar interactions between the two sulfone groups as

$$E_{es} = \mu\mu\,(\cos\theta)/4\pi\epsilon\epsilon_0 r^3 \qquad (3)$$

where $E_{es}$ is the electrostatic energy, $\mu$ is the dipole moment of a sulfone group, and $\theta$ is the angle between the two dipoles. While this neglects intermolecular interactions, it does indicate that the electrostatic contribution to the molecules potential energy is positive when the dipoles are aligned. Thus, this represents an energetically unfavorable state compared to a negative contribution when the dipoles are antialigned, indicating a favorable, more stable configuration. For a free molecule, the size of the electrostatic contribution to the total molecular potential energy can be calculated using eq 3 and is estimated to be approximately 0.135 kcal/mol (using $\mu$ = 1.63 D, $r$ = 5 Å, and $\epsilon$ = 2.25). In order for the molecule to move to a more stable electrostatic configuration, a rotation or twisting (or a gauche defect) must be introduced into the hydrocarbon chain separating the two sulfone groups. The energy required to introduce such a defect will act as a barrier against such a reduction in the electrostatic potential energy. Only if $E_{es}$ is within several kiloteslas of $E_g$ would such a realignment of the dipoles take place for a significant proportion of the molecules. The increase in energy caused by introducing a gauche defect is indeed of the order of $E_{es}$; however, in the case of monolayers one is not dealing with a free molecule and significant intermolecular forces exist, which would act against such a rearrangement of the sulfone dipoles. What is to be emphasized, however, is that there does exist some driving force that lowers the stability of monolayers of V in comparison to those of VI and, therefore, may contribute to the disorder found in monolayers of V. The move to higher energies of the sulfone asymmetric stretch for monolayers of VI may be attributed to enhanced intermolecular interaction due to the additional sulfone moiety. This is to be studied further by looking at temperature dependence of the IR spectra. It is also noted that the methylene wagging bands associated with the hydrocarbon chain are significantly affected for compounds V and VI. Part of the reason for this may be in the number of $CH_2$ units between the two sulfone groups.

## Conclusions

The introduction of groups with large in-plane dipoles has very little effect on molecular conformation within a monolayer, and the molecules are in the all-trans conformation. In contrast, these in-plane dipoles have a profound effect on molecular tilt; i.e., the molecules tilt in one direction only. Such a molecular tilt is in contrast to that which exists in assemblies of simple alkanethiols on Au(111).[20] Evidently, this molecular tilt is the result of the strong $SO_2\cdots SO_2$ electrostatic interactions that promote the formation of a plane of dipoles within the assembly. Hence, the introduction of a plane of dipoles within the assembly affects the packing and ordering of the monolayers and provides a means by which dipolar interactions within molecular assemblies may be studied.

From the wetting behavior of these films, one finds a general trend that the contact angles decrease as the length of the chain above the sulfone group is reduced. This can be interpreted in two ways: (a) the disorder near the surface could be increasing and/or (b) the dipolar interactions due to the polar sulfone become more prominent. IR data indicate that the disorder resulting from the incorporation of the sulfone groups is the primary cause. In considering the differences in the wetting behavior between these molecules and the regular alkanethiol monolayers, a third factor must also be taken into consideration. Since the polarizability of a hydrocarbon chain is anisotropic, then if such molecules display a *preferred* direction of tilt, they will present a surface with a different degree of polarizability than that obtained from a surface with no preferred direction of tilt. Evidence for such a preferred molecular conformation, within these monolayers, has been established.

The XPS technique can be used to determine the relative positions of specific groups in hydrocarbon monolayers: The monolayers studied here are found to be continuous and have a uniform thickness of 17.7 Å. Also, there is evidence for the reduction of the $SO_2$ group during long exposure to high-energy X-rays, analysis times ca. 15 h.

Finally, it seems quite remarkable that the $SO_2$ groups perturb the monolayer so little relative to the monolayers without them. We feel, however, that ordering effects such as those reported here should not be restricted to sulfone groups only, provided that the size and shape of the interacting groups are comparble to those of a methylene. Clearly, the sulfone groups do perturb in-layer close packing of the alkyl chains due to the introduction of free volume, but this perturbation is compensated by the ordering induced through the dipole–dipole interactions. On the other hand, if a group is too bulky, and there are no ordering mechanisms, it introduces a planar perturbation from close packing that results in a progressive distortion of the alkyl chains propagating from the plane of the perturbation.[4] For examples, this kind of perturbation exists in self-assembled alkanethiol monolayers containing polar aromatic groups, where an even bulkier group was introduced into the chain,[1] and in monolayers of alkanethiols on Au(100), where chemisorption in

a square lattice geometry[34] acts as the perturbing plane. Preliminary molecular dynamics (MD) simulations on these systems show that the introduction of planar perturbation to in-plane hexagonal close packing results in an increase in the intramolecular energy.[4] This increase is mainly in the bond torsional energy and is manifested in a curvature in the alkyl chain, which is still in the all-trans conformation.

The data presented in this paper cannot address the molecular details of the assembly. For that, one has to resort to, for example, normal mode calculations. However, the introduction of a sulfone group into the alkyl chain results in the formation of two alkyl chain assemblies, and their packing and orientation cannot be considered a priori to be the same. Thus, realistic molecular dynamics simulations should be used to address such molecular-level considerations. We are now in the process of developing force field parameters for the chemisorption of alkanethiols on Au(111)[35] and hope to be able to present the results of realistic MD simulations of the systems studied here in the future.

**Acknowledgment.** We thank Prof. Michael Klein of the University of Pennsylvania for providing preprints. R.G.S. gratefully acknowledges support by The National Institutes of Health (Grant GM-27690).

**Supplementary Material Available:** Syntheses of compounds I–VI (6 pages). Ordering information is given on any current masthead page.

(34) Strong, L.; Whitesides, G. M. *Langmuir* **1988**, *4*, 546.

(35) Sellers, H.; Ulman, A.; Shnidman, Y.; Eilers, J. E. Manuscript in preparation.